

Dynamic state switching in nonlinear multiferroic cantilevers

Tiberiu-Dan Onuta,^{1,a),b)} Yi Wang,^{2,a)} Christian J. Long,² Samuel E. Lofland,³ and Ichiro Takeuchi¹

¹Department of Materials Science and Engineering, University of Maryland, College Park, Maryland 20742, USA

²Department of Physics, University of Maryland, College Park, Maryland 20742, USA

³Department of Physics and Astronomy, Rowan University, Glassboro, New Jersey 08028, USA

(Received 20 February 2012; accepted 10 July 2012; published online 26 July 2012)

We demonstrate read-write-read-erase cyclical mechanical-memory properties of all-thin-film multiferroic heterostructured cantilevers when a high voltage is applied on the $Pb(Zr_{0.52}Ti_{0.48})O_3$ piezo-film. The device state switching process occurs due to the presence of a hysteresis loop in the piezo-film frequency response. The reference frequency at which the strain-mediated $Fe_{0.7}Ga_{0.3}$ based multiferroic device switches can also be tuned by applying a DC magnetic field bias that contributes to increase of the cantilever effective stiffness. The switching dynamics is mapped in the phase space of the device measured transfer function characteristic for such high piezo-film voltage excitation, providing additional information on the dynamical stability of the devices. © 2012 American Institute of Physics. [<http://dx.doi.org/10.1063/1.4738991>]

We have previously reported on all-thin-film multiferroic¹ ME (magneto-electric) devices consisting of piezoelectric/magnetostrictive $(Pb(Zr_{0.52}Ti_{0.48})O_3)$ (*PZT*)/ $Fe_{0.7}Ga_{0.3}$ heterostructures on *Si*-micromachined cantilevers^{2,3} (Fig. 1(a)) as miniaturized magnetically driven platforms for magnetic field sensors as well as for efficient magnetic energy harvesters. In such devices, the enhancement of the ME response occurs when the modulation frequency of the external AC magnetic field coincides with the mechanical first-order flexural eigenmode of the cantilevers. Thin-film multilayers also allow engineering of the interface state to optimize coupling at the multiferroic bilayers, thus minimizing interfacial damping. In addition, eddy currents are effectively eliminated in such cantilever devices due to the reduced thickness of the magnetostrictive film. These are important ingredients⁴⁻⁶ for attaining a high *Q*-factor (≈ 2000 in vacuum, magnetically driven mode²) in free-standing ME cantilevers which in turn provides enhanced response at resonance.

Here, we show that efficient coupling between the electric, magnetic, and mechanical degrees of freedom in multiferroic heterostructured sensors/actuators and their strongly nonlinear driving regimes can lead to hysteretic switching of the sensor or actuator response between two states dictated by device parameters. Thus, the dynamics of multiferroic cantilever devices can be utilized for switching their magnetic⁷ or spectral⁸ response. The basic operations of the multiferroic devices are (1) ME transduction of magnetostrictive response due to the AC magnetic field via detection of piezo-signals (magnetically driven mode²); and (2) detection of response due to AC piezo-electric excitation voltage (voltage-driven mode).

In the magnetically driven mode,² the acquired signal is the device ME voltage when the applied AC magnetic field is fixed. In the voltage-driven mode (Fig. 1(b)), the acquired

signal is the current flowing in the circuit, which includes the device implemented in a “current bridge” with a current transformer. In the piezo-voltage-driven mode, no AC magnetic field is applied. By “device signal,” we consider the current flowing through the “current bridge” circuit (Fig. 1(b)) when $C_V = C_S$. The signal contribution of stray capacitance is reduced, and the current signal recorded by the lock-in amplifier is also minimized. Thus, the measured signal includes the contribution only from the device itself and excludes any spurious signals from peripheral sources.

Sweeping the applied DC magnetic field bias, H_{DC} , in both directions shows^{2,9} that the device flexural resonant frequency, $f_R = f_R(H_{DC})$, displays hysteretic (“butterfly” curve) behavior. The response of the multiferroic cantilevers to the H_{DC} sweep is complex, involving a strong shift of the resonant frequency, f_R . Also, when $H_{DC} = 0$, the device resonates at the natural flexural mode, $f_R = f_{R0}$, and the device signal² is not null, behavior that is not observed in the frequency-independent “butterfly” response specific to bulk ME materials/devices.

In the voltage-driven mode, when the ME device is weakly driven by an external piezo-voltage signal, the model of a harmonic oscillator with an external drive and weak near-resonant driving damping can be applied to explain the Lorentzian shape of resonant peaks (Fig. 2, the 50 mV-actuation curve). Upon increasing the actuation voltage, anharmonicity begins to set-in in the oscillator,⁸ broadening the peak shape that eventually becomes a distorted non-Lorentzian one. Moreover, a blue-shift of the resonant peak occurs when the frequency range is increasingly swept, leading to a “hard-spring” non-Hookean behavior (Fig. 2).

A dynamical model for our nonlinear multiferroic cantilever can be established based on the Duffing equation of an excited oscillator with negligible feedback on the external energy source.¹⁰ The Duffing oscillator¹⁰ has both the harmonic restoring force, k_0x , and the cubic nonlinearity, ξx^3 , where x is the cantilever deflection, k_0 is the harmonic spring constant, and ξ is a coefficient. From dynamics standpoint,

^{a)}Tiberiu-Dan Onuta and Yi Wang contributed equally to this work.

^{b)}Author to whom correspondence should be addressed. Electronic mail: tonuta@umd.edu.

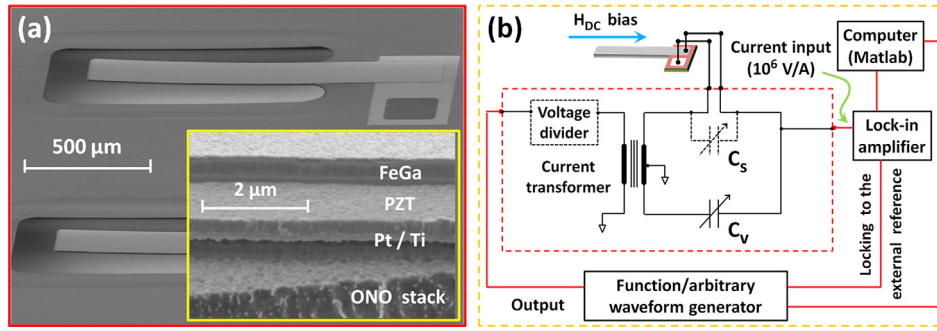


FIG. 1. (a) Scanning electron microscopy (SEM) image of microfabricated all-thin-film multiferroic cantilever devices. The cantilever is 950- μm long, 200- μm wide, and $\sim 5\text{-}\mu\text{m}$ thick. The device wiring regions are at the base of the cantilever (Ref. 2). Inset: Detailed SEM micrograph showing the heterostructure layered edge. (b) Schematic of the experimental setup based on a current bridge platform. C_S is the device stray capacitance, and C_V is an adjustable capacitor for minimizing the device stray capacitance. The cantilever long axis is aligned parallel to H_{DC} . The current transformer is a MET-17 model (Tamura Corp.). The voltage divider ratio is 17.6:1. The measurements are performed in vacuum (3.5×10^{-4} mbar) and with a SR 830 DSP lock-in amplifier.

when $\xi > 0$, the cubic nonlinearity is the cause of the spring constant “hardening” process and the non-Lorentzian blue-shifting (with respect to $f_{R0} \sim \sqrt{k_0}$) of a single frequency-response curve seen^{8,10} in Fig. 2. Thus, the Duffing cantilever can be interpreted as a forced oscillator with an effective spring constant ($k_{eff} = k_{eff,L} + k_{eff,NL}$, where the subscripts stand for linear (L) and nonlinear (NL)). The jumping (or the “fold catastrophe”) phenomenon of the frequency response taking place once the cubic nonlinearity has high dynamical contribution is also the cause of our device displaying multivalued signal amplitude hysteresis.¹⁰

To study the effect of H_{DC} on the behavior of a multiferroic device when a high actuation voltage is applied (on the cantilever electrodes), we generate the plots in Fig. 3 (in the voltage-driven mode). For a fixed H_{DC} and when the direction of the frequency sweep is reversed, a different dynamics takes place. When the driving frequency (which is the PZT-film loading rate) is swept in the both directions, both the frequency dependence of the hysteretic PZT-film

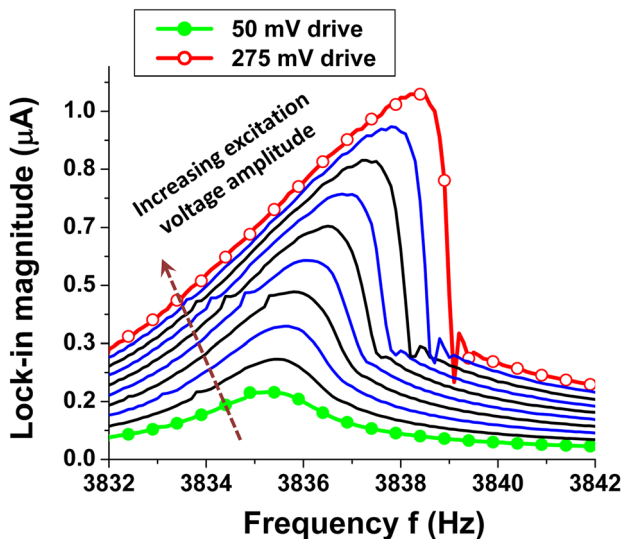


FIG. 2. Lock-in current measurements for a single multiferroic device at $H_{DC} = 0$ when the amplitude of the driving voltage (from a function generator) is increased. In these measurements, the driving frequency is adiabatically increased, enabling quasi-stationary data acquisition. The actuation amplitude is held fixed for each frequency scan. The measured device has $f_{R0} \cong 3835$ Hz.

strain—electric field response and the high-voltage actuation lead to a magnitude-dependent (Fig. 2) nonlinear frequency response of the cantilever first flexural mode (by hardening or, sweep direction dependently, softening the device stiffness, k_{eff} , through $k_{eff,NL}$). When increasing H_{DC} , the position of the hysteresis of the device spectral response blue-shifts. Thus, H_{DC} induces more stress into the magnetostrictive layer that is transferred to the piezoelectric film which in turn leads to the change of k_{eff} but mainly through $k_{eff,L}$.

In order to study the dynamic state switching behavior of the multiferroic cantilever, a time series of the current magnitude of device response is recorded for a certain device driving frequency, $f_{drive}(t)$. The actuation frequency, $f_{drive}(t)$, consists of a fixed (reference) drive frequency, f_{ref} , overlapped with a time series of fast regular frequency changes with peak values of $\Delta f = f - f_{ref}$, where f is chosen arbitrarily on the device spectral response (in the non-hysteretic case, Fig. 4(a)) or outside the projected hysteresis (in the nonlinear case, Fig. 4(b)). The reference frequency, f_{ref} , is usually chosen not to match the resonant frequency, f_R , of the linear device for the corresponding H_{DC} . The multiferroic device is, thus, driven by a piezo-voltage of $V_0 \cos(2\pi f_{drive}(t)t + \varphi)$, with f_{drive} given by the expression

$$f_{drive}(t[s])[Hz] = f_{ref} + \Delta f \cdot \square[t - (10.5T + 2\lambda \cdot 10T)] - \Delta f \cdot \square[t - (21.5T + 2\lambda \cdot 10T)], \quad (1)$$

where V_0 is the drive voltage amplitude, $\square(t)$ is the rectangular function, λ is an integer, and T is 1 s for the data acquisition interval. The frequency, $f_{drive}(t)$, described by Eq. (1) is plotted in Figs. 4(c) and 4(d) (lower curves). Because the carrier driving waveform parameters (the excitation voltage amplitude, V_0 , and the reference frequency, f_{ref}) are maintained at the same values in the proposed frequency switching experiment, from here on we will refer to the fast changes in the studied time series of the actuating frequency as “frequency pulses” (Figs. 4(c) and 4(d), lower curves).

In the device linear regime with a low piezo-voltage excitation (Fig. 4(a)), the working device frequency is set to be at $f_{ref} = 3682$ Hz. A time series of frequency pulses (with the peak values of $\Delta f = 5$ Hz and with the duration of

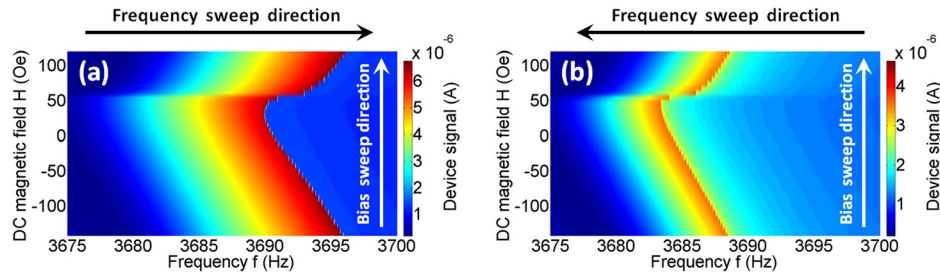


FIG. 3. Mapping the bistable multiferroic device when high amplitude actuation voltage (1 V) is applied for (a) increasing frequency sweep and (b) decreasing frequency sweep. In both cases, H_{DC} is also swept from -125 Oe to 125 Oe. For each H_{DC} , the frequency is swept in both directions. The frequency sweep cycle results in the device hysteretic behavior within the high voltage-driven regime and in the presence of H_{DC} . The measured device (that is different from the one used to generate the plot in Fig. 2) has $f_{R0} \cong 3681$ Hz. The discontinuity regions present in the plots are due to the magnetization switching. The linear dependence $f_R = f_R(H_{DC})$ can be explained as a result of the interplay of Zeeman and anisotropy energies (Refs. 2 and 9).

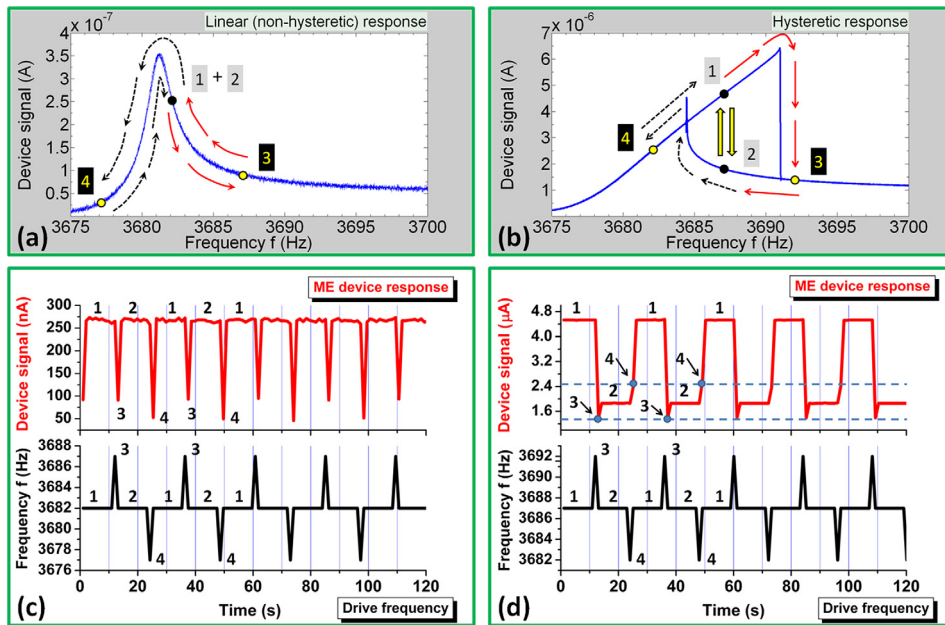


FIG. 4. Hysteretic multiferroic device in the frequency switching regime at $H_{DC} = 0$. (a) Non-hysteretic ME device response to low voltage excitation (for 50 mV drive). (b) Hysteretic response of the ME device to high voltage actuation corresponding to the situation from Fig.3 (for 1 V drive). (c) Non-switching behavior of the device in linear regime. (d) ME bistable response (upper curve) to a pulse-like frequency drive (lower curve) in the hysteretic regime, displaying the frequency switch.

$T = 1$ s) is applied on the reference actuation signal. The multiferroic device proceeds from a dynamic stable state 1 to another stable state 2 through the metastable device states 3 and 4, but there is no state switching feature in the device dynamics (the arrows in Fig. 4(a) indicate the directions of the device frequency jumps among different states) due to the lack of a spectral hysteresis. In the linear case, the defined “high” and “low” stable states 1 and 2 coincide at the given reference frequency (Fig. 4(c)).

Reversing the frequency sweep direction leads to hysteretic multiferroic device behavior in the high piezo-voltage-driven mode (Fig. 4(b)). This time the chosen device reference frequency is $f_{ref} = 3687$ Hz, which is shifted with respect to f_{ref} chosen in the linear case, due to the device spring constant hardening. The variation of the multiferroic cantilever $k_{eff,NL}$ -spring constant results in the resonant peak shifting and hysteretic bistability.⁸ As in the linear case, the frequency pulses have the same peak values of $\Delta f = 5$ Hz and the same duration, $T = 1$ s. Starting from a stable “high” device signal level (device upstate 1), a switching process to another stable “low” state (device state 2) is possible by applying a narrow 5 Hz-peak frequency pulse. The device is temporarily in a metastable state (device state 3) and then settles on the stable downstate 2. Applying a reverse

frequency pulse (with the same peak value, $\Delta f = 5$ Hz, and with the same width of 1s) to f_{ref} , the device proceeds back on the initial stable state (device upstate 1) though an intermediate (temporary) metastable state (device state 4). The frequency switch causes latching in one of two possible configurations: upstate 1 and downstate 2 (Figs. 4(b) and 4(d)). Thus, an implementation of a memory bit can be achieved by setting or resetting the logic bit with frequency pulses. The way to achieve the stable states is shown with arrows in Fig. 4(b). The state positions are indicated in the time series of both the ME device response and f_{drive} (Fig. 4(d)). An equivalent way to describe the switching experiment of our multiferroic device is as a bit logic memory process of “read(1)-write(3)-read(2)-erase(4)” induced by the applied piezo-voltage, $V_0 \cos(2\pi f_{drive}(t)t + \varphi)$. The reference frequency, f_{ref} , at which the logic memory process is implemented in the multiferroic device (Figs. 4(b) and 4(d)) can be tuned by changing the spectral hysteresis position using the applied H_{DC} (Fig. 3).

A common way to analyze the characteristics of a non-linear oscillator is plotting its dynamics in a “phase space” (Fig. 5). For our multiferroic cantilever devices, one way to represent a phase space is to plot the acquired signal, $S = S(f_{drive})$, with respect to its derivative, dS/df_{drive}

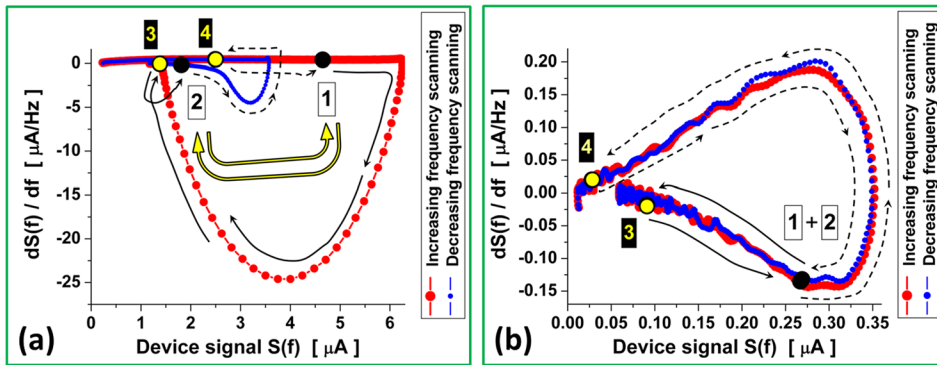


FIG. 5. Multiferroic cantilever dynamics in the transfer function “phase-space” representation at $H_{DC} = 0$. (a) Switching process in the phase-space hysteresis. (b) Linear case when the lack of device hysteretic behavior leads to a non-switching device response. The manifold cusps are consequences of limited frequency scan range in the experiments.

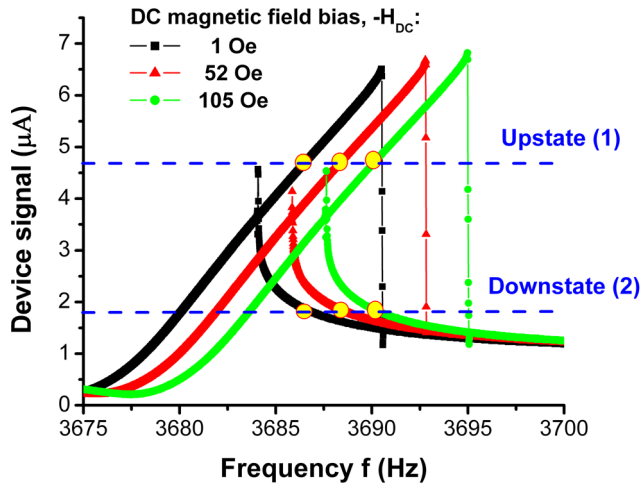


FIG. 6. Frequency-response hysteresis loop translation when different ($-H_{DC}$) is applied. Consequently, the frequency, f_{ref} , at which the switch takes place can be tuned, while switching states can be held at the same signal values, due to only the dependence $k_{eff,L} = k_{eff,L}(H_{DC})$, (Ref. 11).

(Fig. 5). The significance of $S(f_{drive})$ is the measured device transfer function. The device hysteretic behavior can be studied by analyzing the phase space topology for different driving modes dictated by the direction of the frequency sweep. The transfer function “phase space” representation is particularly instrumental in understanding the stability of device dynamics in different device circuit configurations. In the nonlinear case with high piezo-film excitation (Fig. 5(a)), the phase space trajectories have a broken symmetry, indicative of a “jump” dynamics (specific to a saddle-node bifurcation) and can be characterized by different “homoclinics” with cusps. When the multiferroic device dynamics is linear (Fig. 5(b)), the phase space trajectories are both symmetrical (overlapped) manifolds with cusps. In both linear and nonlinear modes, the phase space manifolds change their positions with the applied H_{DC} .

Our cantilever response in switching processes shows threefold possibilities to tune the position of the spectral hys-

teresis and the reference frequency, f_{ref} , at which the switch can be induced: changing the actuation piezo-film voltage (Figs. 4 and 5), varying H_{DC} (and, implicitly, the device linear $k_{eff,L}$ -spring constant¹¹), (Fig. 3) and engineering the device geometrical parameters (Fig. 1). Changing the excitation voltage magnitude will not preserve the position of the device switching states due to the fact that both shape and area of the response hysteresis change (Fig. 2). The multiferroic cantilever system presents an advantage over the other types of mechanical memory switches such as the frequency at which the switch works can be tuned by H_{DC} , and the switching positions can be held at the same signal values on a relatively large spectral spanwise response (Fig. 6).

Fabrication was performed at the Cornell Nano-Scale Science and Technology Facility (CNF) and Maryland Nanocenter Fablab. SEM images were taken at NISP Lab of the Maryland Nanocenter. Research was supported by DARPA HUMS Program (DARPA DSO FA86500917944), partially supported by ARO W911NF-07-1-0410, UMD-NSF-MRSEC (DMR 0520471), and NEDO. S.E.L. acknowledges support from NSF Grant 0927326. We acknowledge the staff from the FabLab and CNF for valuable discussions.

¹M. Fiebig, *J. Phys. D: Appl. Phys.* **38**, R123–R152 (2005).

²T. D. Onuta, Y. Wang, C. J. Long, and I. Takeuchi, *Appl. Phys. Lett.* **99**, 203506 (2011).

³P. Zhao, Z. L. Zhao, D. Hunter, R. Suchoski, C. Gao, S. Mathews, M. Wuttig, and I. Takeuchi, *Appl. Phys. Lett.* **94**, 243507 (2009).

⁴R. C. O’Handley, J. K. Huang, D. C. Bono, and J. Simon, *IEEE Sens. J.* **8**, 57–62 (2008).

⁵H. Greve, E. Woltermann, H. J. Quenzer, B. Wagner, and E. Quandt, *Appl. Phys. Lett.* **96**, 182501 (2011).

⁶Y. J. Wang, D. Gray, D. Berry, J. Q. Gao, M. H. Li, J. F. Li, and D. Viehland, *Adv. Mater.* **23**, 4111 (2011).

⁷Y. J. Chen, T. Fitchorov, C. Vittoria, and V. G. Harris, *Appl. Phys. Lett.* **97**, 052502 (2010).

⁸W. J. Venstra, H. J. R. Westra, and H. S. J. van der Zant, *Appl. Phys. Lett.* **97**, 193107 (2010).

⁹P. von Lockette, S. E. Lofland, J. Biggs, J. Roche, J. Mineroff, and M. Babcock, *Smart Mater. Struct.* **20**, 105022 (2011).

¹⁰A. H. Nayfeh and D. T. Mook, *Nonlinear oscillations* (Wiley, 1995).

¹¹A. J. Dick, B. Balachandran, D. L. DeVoe, and C. D. Mote, *J. Micromech. Microeng.* **16**, 1593–1601 (2006).